Perturbing the DNA Sequence Selectivity of Metallointercalator−Peptide Conjugates by Single Amino Acid Modification†

Curtis A. Hastings and Jacqueline K. Barton*

Division of Chemistry and Chemical Engineering, California Institute of Technology, Pasadena, California 91125

Received August 24, 1998; Revised Manuscript Received June 4, 1999

ABSTRACT: Metallointercalator−peptide conjugates that provide small molecular mimics to explore peptide−nucleic acid recognition have been prepared. Specifically, a family of peptide conjugates of $[Rh(phi)_2(phen')]^{3+}$ [where phi = 9,10-phenanthrenequinone diimine and phen′ = 5-(amidoglutaryl)-1,10-phenanthroline] has been synthesized and their DNA-binding characteristics examined. Single amino acid modifications were made from the parent metallointercalator−peptide conjugate $[Rh(phi)_2(phen')]^{3+}$-AANVAIAAWERAA-$CONH_2$, which targets 5′-CCA-3′ site-specifically. Moving the glutamate at position 10 in the sequence of the appended peptide to position 6 {$[Rh(phi)_2(phen')]^{3+}$-AANVAEAAWARAA-$CONH_2$} changed the sequence preference of the metallointercalator−peptide conjugate to 5′-ACA-3′. Subsequent mutation of the glutamate at position 6 to arginine {$[Rh(phi)_2(phen')]^{3+}$-AANVARAAWARAA-$CONH_2$} caused more complex changes in DNA recognition. Thermodynamic dissociation constants were determined for these metallointercalator−peptide conjugates by photoactivated DNA cleavage assays with the rhodium intercalators. At 55 °C in the presence of 5 mM $MnCl_2$, $[Rh(phi)_2(phen')]^{3+}$-AANVAIAAW-ERAA-$CONH_2$ binds to a 5′-CCA-3′ site with $K_d = 5.7 \times 10^{-8}$ M, whereas $[Rh(phi)_2(phen')]^{3+}$-AANVAEAAWARAA-$CONH_2$ binds to its target 5′-ACA-3′ site with $K_d = 9.9 \times 10^{-8}$ M. The dissociation constant for $[Rh(phi)_2(phen')]^{3+}$ with random-sequence DNA is 7.0×10^{-7} M. Structural models have been developed and refined to account for the observed sequence specificities. As with much larger DNA-binding proteins, with these metal−peptide conjugate mimics, single amino acid changes can lead to single or multiple base changes in the DNA site targeted.

DNA binding proteins play important regulatory roles in replication, transcription, and repair of the genome. Consequently, there has been significant interest in the molecular basis of their sequence selectivity. No simple set of rules correlates the amino acid sequences of DNA binding proteins with the nucleotide sequences of their targets (*1, 2*). Crystallographic studies of protein−DNA complexes have revealed that multiple amino acids may be used to recognize a given base, and multiple bases may be recognized by the same amino acid. Mutagenesis experiments with zinc finger transcription factors have demonstrated that the sequence selectivity of these proteins may be altered by introducing mutations at critical positions. In many cases concerted amino acid changes are required to obtain new sequence selectivity, and single amino acid changes can alter the DNA sequence selectivity at multiple positions of the DNA target (*3*−*7*). Thus, combinatorial approaches provide effective methods for obtaining oligopeptides that target specific nucleotide sequences (*8*). An improved understanding of protein−DNA interaction would find application in the design of repressors, transcription factors, and nucleases with altered sequence selectivity.

One of the focuses of our laboratory has been in the development of peptide conjugates of rhodium(III) complexes as models for sequence-selective DNA binding proteins (*9*−*11*). The intercalating phi complexes of rhodium bind double helical DNA from the major groove with high affinity ($K_d = 10^{-6}$ M) (*12*). Thus, the rhodium complex serves to deliver the peptide to the DNA recognition site. This approach offers the opportunity to explore site-specific recognition of DNA by small peptides (11−15 aa) where residues may be varied in a systematic and well-defined fashion. Moreover, the phi complexes of rhodium cleave DNA upon photoactivation, permitting site selectivity to be assayed with high resolution.

Previously, we reported that tethering oligopeptides derived from the recognition α-helix of the *434* repressor to the relatively sequence-neutral metallointercalator $[Rh(phi)_2(phen')]^{3+}$ [where phen′ = (5-amidoglutaryl)-1,10-phenanthroline][1] partially conferred the sequence selectivity of the parent protein on the metallointercalator (*11*). Oligopeptides derived from the recognition α-helix of the P_{22} repressor, when tethered to $[Rh(phi)_2(phen')]^{3+}$, afforded sequence-selective recognition of 5′-CCA-3′ sequences (*9*). The highest DNA site specificity (ratio of photocleavage at target sequences to total photocleavage) was obtained with $[Rh(phi)_2(phen')]^{3+}$-AANVAIAAWERAA-$CONH_2$ ([Rh]−E10). [Rh]−E10 is shown schematically in Figure 1. Previous work has indicated that Glu^{10} is an essential determinant of

† We are grateful to the NSF (Grant CHE-9422547) for financial support of this work. C.A.H. thanks W. R. Grace & Co. for a summer research fellowship.

* To whom correspondence should be addressed.

[1] Abbreviations: phi, 9,10-phenanthrenequinone diimine; phen′, 5-(amidoglutaryl)-1,10-phenanthroline; TFE, trifluoroethanol.

10.1021/bi982039a CCC: $18.00
Published on Web 07/16/1999

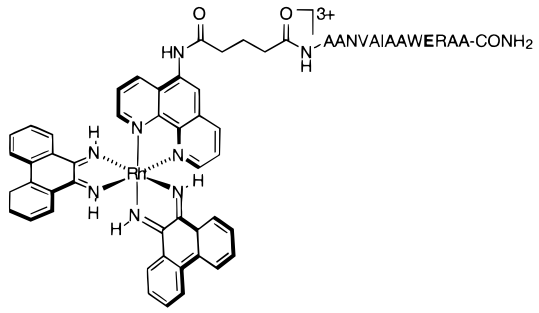

Conjugate	Peptide Sequence
[Rh]-E6	AANVA**E**AAWARAA-$CONH_2$
[Rh]-E7	AANVAI**E**AWARAA-$CONH_2$
[Rh]-E8	AANVAIA**E**WARAA-$CONH_2$
[Rh]-E10	AANVAIAAW**E**RAA-$CONH_2$
[Rh]-E12	AANVAIAAWAR**E**AA-$CONH_2$
[Rh]-E13	AANVAIAAWARA**E**AA-$CONH_2$
[Rh]-E6E10	AANVA**E**AAW**E**RAA-$CONH_2$
[Rh]-R6A10	AANVA**R**AAWA**R**AA-$CONH_2$
[Rh]-R6E10	AANVA**R**AAW**E**RAA-$CONH_2$
[Rh]-I6A10	AANVA**I**AAWA**R**AA-$CONH_2$

FIGURE 1: Metallointercalator−peptide conjugates. The parent metallointercalator−peptide conjugate, [Rh]−E10, is shown schematically with Glu^{10}, which makes base-specific contacts with the DNA target of [Rh]−E10, indicated in boldface type. Amino acid sequences for the family of conjugates prepared in this study are shown below.

the 5′-CCA-3′ sequence selectivity of [Rh]−E10 and related metallointercalator−peptide conjugates. Mutation of Glu^{10} to alanine or aspartate abolished specificity. Systematic mutation of amino acid residues other than Glu^{10} did not significantly alter the sequence selectivity of the parent metallointercalator−peptide conjugate. Instead, diminished specificity was observed with mutations that reduce the helical content of the peptide. Moreover, the helical content of P_{22} repressor-derived peptides is highly dependent on the residue at position 10. From these results, Sardesai et al. proposed a "glutamate switch" model for 5′-CCA-3′ recognition by P_{22} repressor-derived metallointercalator−peptide conjugates (*11*). Only glutamate both confers high helical content on the peptide and makes specific interactions with the DNA target. Consequently, specific recognition is only observed with peptides that contain glutamate at position 10. It is interesting to note that [Rh]−E10 does not recognize the same nucleotide sequences as the P_{22} repressor, from which it was derived; instead the corresponding glutamate in P_{22} is involved in hydrogen-bonding contacts within the protein interior. We sought to examine the thermodynamic basis for the sequence selectivity of [Rh]−E10 in more detail and to develop a family of metallointercalator−peptide conjugates based on [Rh]−E10 that exhibited a variety of sequence preferences. We examined peptides in which the position of the essential glutamate was varied relative to the other amino acid residues. Here we describe novel recognition elements obtained by such modification.

MATERIALS AND METHODS

Materials. Sonicated calf thymus DNA was purchased from Pharmacia. Plasmid pUC18 was purchased from Boehringer-Mannheim. All enzymes utilized were from New England Biolabs or Boehringer-Mannheim. [α-^{32}P]dATP and [γ-^{32}P]ATP were obtained from NEN−Dupont. Oligonucleotides were synthesized by the phosphoramidite method (*13*) with 1.0 μmol columns on an Applied Biosystems ABI392 DNA/RNA synthesizer.

Instrumentation. Nucleic acids and metallointercalator−peptide conjugates were purified on a Waters 600 multisolvent delivery system equipped with a 996 PDA detector, Vydac 218TP510 (metallointercalator−peptide conjugates) or Rainin Dynamax 300-Å (DNA) semipreparative C_{18} columns, and Millennium chromatography manager software. CD spectra were recorded on a Jasco J-500 or J-600 spectrometer with 1 cm path length cells. UV−visible spectra were recorded on an HP-8452A diode array spectrometer. Photocleavage experiments were performed with an Oriel model 6140 1000 W Hg/Xe lamp fitted with a monochromator and a 300 nm cutoff filter. Gel electrophoresis experiments were quantified by use of a Molecular Dynamics Phosphorimager and ImageQuant software.

Synthesis and Characterization of Metallointercalator−Peptide Conjugates. Peptide conjugates of $[Rh(phi)_2(phen')]^{3+}$ were synthesized as described by Sardesai et al. (*9*, *10*). Peptide conjugates of $[Rh(phi)_2(phen')]^{3+}$ were characterized by MALDI-TOF mass spectroscopy. Observed and calculated molecular ion peaks (in parentheses) were as follows: [Rh]−E6, 2074.5 (2074.1); [Rh]−E7, 2117.4 (2117.2); [Rh]−E8, 2119.9 (2116.2); [Rh]−E12, 2189.3 (2187.3); [Rh]−E13, 2259.3 (2260.3); [Rh]−E6E10, 2132.9 (2132.1); [Rh]−R6A10, 2102.1 (2101.2); [Rh]−R6E10, 2160.7 (2159.2).

Photocleavage of DNA Restriction Fragments. Plasmid pUC18 was digested with *Eco*RI restriction endonuclease, treated with calf intestinal alkaline phosphatase, and 5′-end-labeled with T4 polynucleotide kinase and [γ-^{32}P]ATP. Alternatively, following digestion with *Eco*RI restriction endonuclease, the plasmid was 3′-end-labeled by treatment with the Klenow fragment of DNA polymerase I and [α-^{32}P]-ATP, dCTP, dGTP, and dTTP. Following 3′- or 5′-end-labeling, the DNA was digested with *Pvu*II restriction endonuclease, yielding labeled fragments of 180 and 140 base pairs. The 180 base pair fragment was isolated by 6% nondenaturing polyacrylamide gel electrophoresis followed by electroelution (*14*, *15*).

Photocleavage reactions were performed in 20 μL total volume contained in 1.7 mL presiliconized Eppendorf tubes. The reaction mixtures contained ~100 000 cpm labeled restriction fragment, 15 μM base pairs sonicated calf thymus DNA, 1 μM metallointercalator, 5 mM $MnCl_2$, and 50 mM pH 7.0 sodium cacodylate buffer. The reaction mixtures were incubated at 55 °C for 5 min and irradiated with 313 nm light at 55 °C for 10 min. Control reactions lacking metallointercalator were irradiated under identical conditions. Following irradiation, 50 μL of 7.5 M aqueous NH_4OAc and 200 μL of EtOH were added. The DNA was isolated by precipitation and washed with cold 80% aqueous EtOH. The precipitated DNA was dried and resuspended in 5 μL of 80% formamide sequencing loading buffer. Approximately 20 000

cpm of each sample, and Maxam−Gilbert A + T and C + G sequencing reactions (*14*, *15*), were loaded on a 6% denaturing polyacrylamide gel and electrophoresed at 1200 V for 2.5 h. The gel was transferred to paper and dried prior to autoradiography.

Quantitation of Photocleavage of DNA Restriction Fragments. Following autoradiography with a Molecular Dynamics Phosphorimager, the photocleavage intensities at each base were measured by volume integration by use of the program ImageQuant. All quantitation was normalized to reflect the same total counts per lane. To correct for variations in photocleavage intensity arising from sequence preferences of the metallointercalator, sequence-dependent variations in photocleavage intensity by the metallointercalator, and light damage to the DNA, the photocleavage intensities at each base in the presence of the metallointercalator were also measured by volume integration. At each base step, the quantitation was performed with identically sized boxes. The percentage change in the photocleavage intensity at each base (ΔI) as a result of the presence of the peptide was then determined to be $(I_{pep} - I_{met})/I_{met}$, where I_{pep} is the photocleavage intensity in the presence of the metallointercalator−peptide conjugate and I_{met} is the photocleavage intensity in the presence of the metallointercalator.

Photocleavage of Oligonucleotides. Oligonucleotides were 5′-end-labeled with T4 polynucleotide kinase and [γ-^{32}P]ATP and hybridized by annealing with a 10-fold excess of the complementary strand. The labeled duplex was purified by 20% nondenaturing polyacrylamide gel electrophoresis and isolated from the gel by the crush and soak method.

Photocleavage reactions were performed in 20 μL total volume contained in 1.7 mL presiliconized Eppendorf tubes. Reaction samples contained ∼100 000 cpm labeled oligonucleotide, unlabeled oligonucleotide and metallointercalator at the indicated concentrations, 5 mM $MnCl_2$, and 50 mM pH 7.0 sodium cacodylate buffer. The reaction mixtures were incubated at 55 °C for 5 min and irradiated with 313 nm light at 55 °C for 10 min. Control reactions lacking metallointercalator were irradiated under identical conditions. Following irradiation, 50 μL of 7.5 M aqueous NH_4OAc and 200 μL of EtOH were added. The DNA was isolated by precipitation and washed with cold 80% aqueous EtOH. The precipitated DNA was dried and resuspended in 5 μL of 80% formamide sequencing loading buffer. Approximately 20 000 cpm of each sample and Maxam−Gilbert A + T and C + G sequencing reactions (*14*, *15*) were loaded on a 20% denaturing polyacrylamide gel and electrophoresed at 1200 V for 2.5 h.

Dissociation Constant Determinations by Photocleavage Titration. Hairpin oligonucleotides were 5′-end-labeled with T4 polynucleotide kinase and [γ-^{32}P]ATP (*16*−*18*). Photocleavage reactions were performed in 20 μL of total volume contained in 1.7 mL presiliconized Eppendorf tubes. The reaction mixtures contained ∼200 000 cpm labeled hairpin oligonucleotide, metallointercalator−peptide conjugate and unlabeled hairpin oligonucleotide in a 1:3 ratio, 5 mM $MnCl_2$, and 50 mM pH 7.0 sodium cacodylate buffer. Metallointercalator−peptide conjugate concentrations ranged from 7.2×10^{-6} to 7.2×10^{-11} M. The reaction mixtures were incubated at 23 or 55 °C for 5 min and irradiated with 313 nm light at 23 or 55 °C, respectively, for 10 min. Control reactions lacking metallointercalator were irradiated under identical conditions, and control reactions containing metallointercalator were incubated at 23 or 55 °C without irradiation. Following irradiation, the reaction mixtures were concentrated in vacuo and resuspended in 5 μL of 80% formamide sequencing loading buffer. Approximately 50 000 cpm of each sample and Maxam−Gilbert A + T and C + G sequencing reactions (*14*, *15*) were loaded on a 20% denaturing polyacrylamide gel and electrophoresed at 1200 V for 2.5 h. The experimental dissociation constants and photocleavage efficiencies (γ) were determined by fitting the observed fraction cleaved (F_c) at the site of interest as a function of DNA $[DNA]_t$ and metallointercalator−peptide conjugate $[L]_t$ concentration to eq 1 (*16*−*18*) by nonlinear regression using SigmaPlot (Jandel Scientific):

$$F_c = (\gamma([DNA]_t + [L]_t + K_d - (([DNA]_t + [L]_t + K_d)^2 - 4[DNA]_t[L]_t)^{1/2}))/(2[DNA]_t) \quad (1)$$

Molecular Modeling. Molecular mechanics calculations were performed with the CVFF force field (*19*). Minimization involved 1000 iterations of steepest descents minimization followed by 1000 iterations (1 ps) dynamics with temperature of 300 K and 5000 iterations of steepest descents minimization. The DNA and the intercalator were fixed throughout the calculation. An ensemble of structures was generated in this fashion.

RESULTS

Cleavage of Restriction Fragments by Metallointercalator−Peptide Conjugates. A family of metallointercalator−peptide conjugates derived from [Rh]−E10 was prepared and characterized. Here, all amino acid substitutions are indicated relative to the sequence of [Rh]−E10 (H_2N-AANVAIAAW-ERAA-$CONH_2$). Derivatives include [Rh]−E6 (I6E, E10A), [Rh]−E7 (A7E, E10A), [Rh]−E8 (A8E, E10A), [Rh]−E12 (A12E, A14), and [Rh]−E13 (A13E, A14, A15). This family was screened for sequence-selective DNA photocleavage by use of the ^{32}P-end-labeled *Eco*RI/*Pvu*II 180-mer restriction fragment of pUC18 (Figure 2). Photocleavage reactions were conducted at 55 °C in the presence of 5 mM $MnCl_2$. These conditions result in optimal affinity and specificity of [Rh]−E10 for its target site. As can be seen in Figure 2, new sequence selectivity was observed with [Rh]−E6. Conversely, [Rh]−E7, [Rh]−E8, [Rh]−E12, and [Rh]−E13 did not afford cleavage patterns that were discernibly different from that of $[Rh(phi)_2(phen')]^{3+}$. On the 5′-end-labeled strand, enhanced cleavage by [Rh]−E6 is observed at A^{62}, A^{64}, and A^{67} of the sequence 5′-C^{58}CAC**A**C**A**AC**A**TAC^{70}-3′ (numbering refers to positions of the complementary base on the 3′-strand). Similarly, cleavage by [Rh]−E6 on the 3′-end-labeled strand is more pronounced at the three adenosine bases of the sequence 5′-T^{38}TTC**A**C**A**C**A**^{30}-3′, whereas cleavage by $[Rh(phi)_2(phen')]^{3+}$ is more pronounced at the cytosines. As with [Rh]−E10, enhanced cleavage is not observed on the complementary strand under the experimental conditions. Significantly, enhanced cleavage by [Rh]−E6 is not observed at other 5′-pur-pyr-pur-3′ sequences. Thus, the consensus sequence for DNA recognition by [Rh]−E6 that emerges from analysis of the cleavage patterns observed with the *Eco*RI/*Pvu*II 180-mer restriction fragment of pUC18 is 5′-AC**A**-3′ (cleavage at the highlighted adenine).

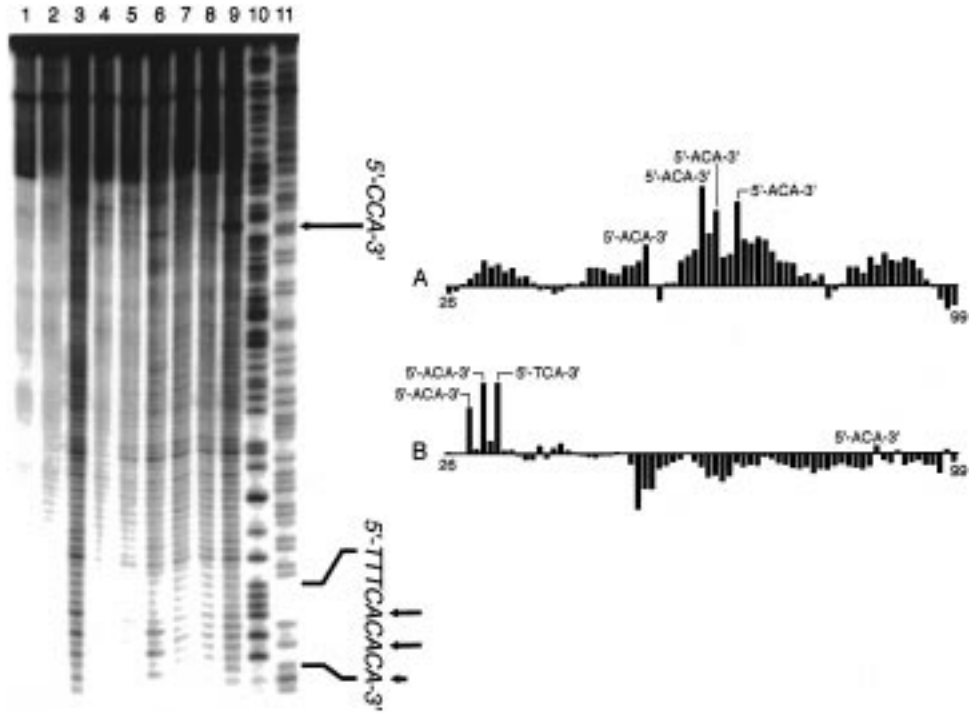

FIGURE 2: (Left) Autoradiogram of a 6% denaturing gel showing photocleavage reactions of the 180 base pair 3′-[^{32}P]-end-labeled *Eco*RI/*Pvu*II fragment of plasmid pUC18. The reaction samples were incubated for 10 min at 55 °C and irradiated for 10 min at 55 °C in the presence of 5 mM $MnCl_2$: lane 1, DNA control; lane 2, fragment irradiated in the absence of rhodium complex; lanes 3−9, fragment irradiated in the presence of 1 μM $[Rh(phi)_2(phen')]^{3+}$, [Rh]−E8, [Rh]−E12, [Rh]−E6, [Rh]−E7, [Rh]−E13, and [Rh]−E10, respectively; lanes 10 and 11, Maxam−Gilbert C + T and A + G sequencing reactions, respectively. (Right) Histograms summarizing cleavage of 3′- and 5′-[^{32}P]-end-labeled restriction fragments by [Rh]−E6 (A, 5′-labeled; B, 3′-labeled). Histograms represent cleavage by peptide conjugates relative to cleavage by $[Rh(phi)_2(phen')]^{3+}$ at each base (see Materials and Methods).

Several features are noteworthy: (i) the observation of sequence-selective DNA cleavage only when a glutamate residue is located at position 6 or position 10 is consistent with our previous observation that the DNA sequence specificity of [Rh]−E10-derived metallointercalator−peptide conjugates correlates with their helical content as measured by circular dichroism spectroscopy (*9*); (ii) the photocleavage efficiency of all of the metallointercalator−peptide conjugates studied is comparable, suggesting that, as shown for [Rh]−E10 (*4*, *5*), the peptide exists in an extended conformation and does not interact with the metal center; and (iii) cleavage on only one of the two strands suggests that the metal complex is canted to one side of the intercalation site (*12*); a similar strand asymmetry was apparent with [Rh]−E10 (*9*).

Photocleavage results with metallointercalator−peptide conjugates derived from [Rh]−E10 by systematically varying the position of Glu^{10} suggested that the amino acids at positions 6 and 10 of these conjugates make base-specific contacts with the DNA. Therefore, the effects of further amino acid changes at these positions were investigated in a second generation of metallointercalator−peptide conjugates. In addition to exploring the sequence selectivity that could be achieved with various combinations of alanine, glutamate, and isoleucine at positions 6 and 10, the effects of arginine substitution at position 6 were investigated. Base-specific contacts between the arginine side chain and thymine and guanine nucleotides are common in crystal structures of transcription factor−DNA complexes (*1*, *2*). Moreover, we envisioned that the positive charge associated with the guanidinium group of arginine would increase the overall affinity of the metallointercalator−peptide conjugates for DNA. A second family of metallointercalator−peptide conjugates was therefore synthesized; this family included [Rh]−E6E10 (I6E), [Rh]−I6A10 (E10A), [Rh]−R6E10 (I6R), and [Rh]−R6A10 (I6R, E10A).

This family of metallointercalator−peptide conjugates was screened for sequence-selective DNA photocleavage as before (Figure 3). Photocleavage by [Rh]−R6A10 was more pronounced than photocleavage by $[Rh(phi)_2(phen')]^{3+}$ at several positions along both strands of the pUC18 180-mer. However, none of the other metallointercalator−peptide conjugates afforded cleavage patterns that were discernibly different from that of $[Rh(phi)_2(phen')]^{3+}$. Analysis of the sequences flanking the sites of enhanced cleavage by [Rh]−R6A10 does not reveal a clear three-base-pair consensus sequence, yet new selectivity, distinct from that observed with [Rh]−E6 and [Rh]−E10, is apparent. Specifically, enhanced cleavage is found on the 5′-end-labeled strand at sites 5′-TC**A**^{52}-3′ and 5′-GC**A**^{82}-3′ and to a smaller extent at 5′-TA**A**^{120}-3′. At the two-base level, the consensus sequence appears still to be 5′-C**A**-3′, but in contrast to the other conjugates examined, enhanced photocleavage is observed with [Rh]−R6A10 at 5′-GC**A**-3′ and 5′-TC**A**-3′. In addition, while [Rh]−E6 and [Rh]−E10 cleave exclusively with 5′-asymmetry, photocleavage by [Rh]−R6A10 occurs with variable asymmetry.

Cleavage of Oligonucleotides by Metallointercalator−Peptide Conjugates. To confirm that the preferred binding site of [Rh]−E6 is 5′-AC**A**-3′, photocleavage of a 31-mer oligonucleotide containing all four possible 5′-NCA-3′ sequences separated by 5′-CGAG-3′ spacers was investigated. Photocleavage reactions were conducted at a range of concentrations in metallointercalator−peptide conjugate

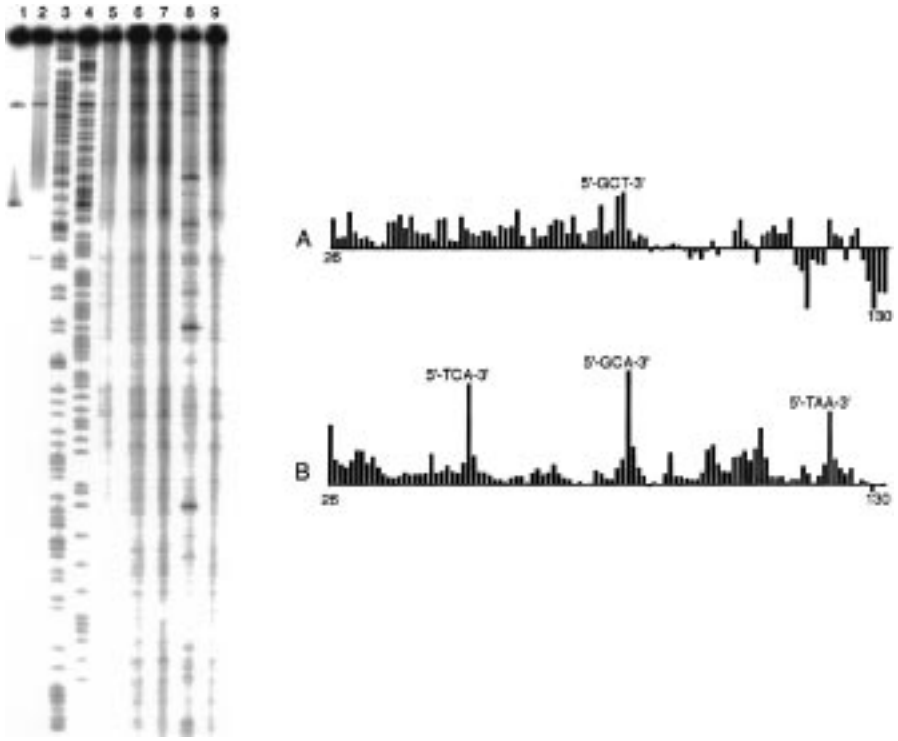

FIGURE 3: (Left) Autoradiogram of a 6% denaturing gel showing photocleavage reactions of the 180 base pair 5′-[^{32}P]-end-labeled *Eco*RI/*Pvu*II fragment of plasmid pUC18. The reaction samples were incubated for 10 min at 55 °C and irradiated for 10 min at 55 °C in the presence of 5 mM $MnCl_2$: lane 1, DNA control; lane 2, fragment irradiated in the absence of rhodium complex; lanes 3 and 4, Maxam−Gilbert C + T and A + G sequencing reactions, respectively; lanes 5−9, fragment irradiated in the presence of 1 μM $[Rh(phi)_2(phen')]^{3+}$, [Rh]−I6A10, [Rh]−E6E10, [Rh]−R6A10, and [Rh]−R6E10, respectively. (Right) Histograms summarizing cleavage of 3′- and 5′-[^{32}P]-end-labeled restriction fragments by [Rh]−R6A10 (A, 3′-labeled; B, 5′-labeled). Histograms represent cleavage by peptide conjugates relative to cleavage by $[Rh(phi)_2(phen')]^{3+}$ at each base (see Materials and Methods).

and unlabeled oligonucleotide. At concentrations below the intercalative dissociation constant of $[Rh(phi)_2(phen')]^{3+}$ for random-sequence DNA, photocleavage by [Rh]−E6 is most intense at the 5′-AC**A**-3′ site. Weak photocleavage is observed at the 5′-TC**A**-3′ site. Quantitation of the photocleavage at the 3′-terminal adenine of the four 5′-NCA-3′ sequences suggests that [Rh]−E6 binds approximately 1.5-fold more tightly to 5′-ACA-3′ than to the other 5′-NCA-3′ sites, corresponding to the small energy difference of approximately 0.3 kcal·mol^{-1}. This analysis assumes that the photocleavage efficiency is equivalent at all four 5′-NCA-3′ sites. For comparison, little difference in the photocleavage intensity at the four 5′-NCA-3′ sequences is observed with $[Rh(phi)_2(phen')]^{3+}$. Under these conditions, [Rh]−E10 cleaves strongly at the 5′-CC**A**-3′ site. Photocleavage by [Rh]−E10 is slightly stronger than photocleavage by $[Rh(phi)_2(phen')]^{3+}$ at the 5′-GC**A**-3′ site. There is no discernible difference in photocleavage intensity by [Rh]−E10 and $[Rh(phi)_2(phen')]^{3+}$ at the 5′-AC**A**-3′ and 5′-TC**A**-3′ sites.

Photocleavage of the *Eco*RI/*Pvu*II 180-mer restriction fragment of pUC18 by [Rh]−E6E10 is not discernibly different from photocleavage by $[Rh(phi)_2(phen')]^{3+}$. However, the sequence selectivities of [Rh]−E6 and [Rh]−E10 suggest that each of the glutamate residues of [Rh]−E6E10 is capable of making specific contacts with the cytosine bases in a putative 5′-CCA-3′ recognition site. Accordingly, photocleavage of the 31-mer oligonucleotide by [Rh]−E6E10 under varying conditions was investigated. In the absence of Mn^{2+}, [Rh]−E6E10 cleaved at the 5′-CC**A**-3′ site with an intensity similar to that of [Rh]−E10, while sequence-selective cleavage by [Rh]−E6 and [Rh]−R6A10 was not observed. Interestingly, in the absence of Mn^{2+}, cleavage by both [Rh]−E10 and [Rh]−E6E10 was seen at the adenine of the 5′-GC**A**-3′ site.

Circular Dichroism of Metallointercalator−Peptide Conjugates. To explore any correlation between sequence-selective DNA recognition and α-helicity, circular dichroism spectra of the metallointercalator−peptide conjugates were recorded at 23 °C at pH 7.0 in the absence and presence of 5 mM $MnCl_2$, and in 25% TFE (Table 1). Under these conditions, CD spectra consistent with, at most, modest α-helical content are observed for some of the metallointercalator−peptide conjugates. Calculated helical contents range up to 33%. Nonetheless, addition of Mn^{2+} or TFE results in increases in the apparent helical content. Importantly, as we have already described, these additives also increase the specificity of DNA recognition by [Rh]−E10 (*9*). The same increases in specificity were observed for [Rh]−E6. Interestingly, [Rh]−E6E10 has a relatively low helical content, and little change is observed upon addition of Mn^{2+} or TFE. Among the family, the strongest apparent DNA photocleavage pattern (although not highest binding constant, vide infra) is obtained for [Rh]−E10, which displays the highest level of apparent α-helicity. Despite low overall measures of α-helicity, then, some correlation between helical content and site specificity occurs for this family of metallointercalator−peptide conjugates. Possibly, binding to DNA helps to drive greater helicity in these small peptides; the absorption characteristics of the metallointercalators, however, make the characterization of any DNA-promoted stabilization of the α-helix problematic.

Table 1: Helical Content[a] of Peptide Conjugates of $[Rh(phi)_2(phen')]^{3+}$

conjugate (5 μM)	helical content[b] (%)	helical content[c] (%)	helical content[d] (%)
[Rh]−E6	<1	5	8
[Rh]−E7	4	8	7
[Rh]−E8	3	6	8
[Rh]−E10	17	21	24
[Rh]−E12	<1	1	2
[Rh]−E13	5	6	8
[Rh]−E6E10	3	5	5
[Rh]−R6A10	2	8	10
[Rh]−R6E10	4	6	10
[Rh]-I6A10	18	25	33

[a] The helical content is calculated by assuming that a fully helical peptide has a mean residue ellipticity ($[\theta_{222}]$) of −31 500 deg·cm^2·dmol^{-1}; see ref *33*. The mean residue ellipticity is defined as $[\theta_{222}] = 100\theta_{222}/cnl$, where θ_{222} is the ellipticity (millidegrees) measured by CD spectroscopy, c is the peptide concentration (millimolar), n is the number of amino acids in the peptide, and l is the path length (centimeters) of the CD cell; see ref *34*. [b] pH 7.0, 23 °C, 10 mM Tris·HCl. [c] pH 7.0, 23 °C, 5 mM $MnCl_2$, 10 mM Tris·HCl. [d] pH 7.0, 23 °C, 25% TFE, 7.5 mM Tris·HCl.

Thermodynamics of Sequence-Selective DNA Binding by Metallointercalator−Peptide Conjugates. To probe the thermodynamics of sequence-selective DNA binding, dissociation constants of [Rh]−E6 and [Rh]−E10 for their target sequences were determined by photocleavage titration. Hairpin oligonucleotides containing the three-base-pair sites of interest flanked by four base pairs to the 5′-side and five base pairs to the 3′-side were employed to minimize the number of potential intercalation sites for the rhodium complex, while maintaining hybridization under the nanomolar concentrations of the experiment. The concentration of the metallointercalator−peptide conjugates ranged from 7.2×10^{-6} to 7.2×10^{-11} M, with a constant metallointercalator:unlabeled oligonucleotide ratio of 1:3. An autoradiogram of a representative photocleavage titration experiment is shown in Figure 4. Cleavage isotherms were obtained by plotting the fraction of the total counts in each lane that were present in the band representing cleavage at the target base. The isotherms (Figure 5, normalized after fitting to eq 1 by multiplying by the quantity [DNA]/([Rh]γ), which represents the amount of cleavage that would be expected under the experimental conditions if the metallointercalator were completely bound to the DNA) were fit to eq 1, yielding the thermodynamic dissociation constants shown in Table 2. Comparison of the resulting values with the intercalative dissociation constant of $[Rh(phi)_2(phen')]^{3+}$ for random-sequence DNA (7.0×10^{-7} M) permitted estimation of the energetic contributions of the peptides to sequence-specific complex formation. At 55 °C in the presence of 5 mM $MnCl_2$, [Rh]−E6 binds 7-fold more tightly to its target sequences than does $[Rh(phi)_2(phen')]^{3+}$, corresponding to a free-energy difference of 1.3 kcal·mol^{-1}. Under the same conditions, [Rh]−E10 binds 13-fold more tightly to its target sequences than $[Rh(phi)_2(phen')]^{3+}$, corresponding to a free-energy difference of 1.7 kcal·mol^{-1}. [Rh]−E6E10 does not afford sequence-selective DNA cleavage in the presence of $MnCl_2$. Consequently, its dissociation constant was measured in the absence of divalent cations. Under these conditions, [Rh]−E6E10 binds 23-fold more tightly to its target sequences than $[Rh(phi)_2(phen')]^{3+}$, corresponding to a free-energy difference of 2.1 kcal·mol^{-1}.

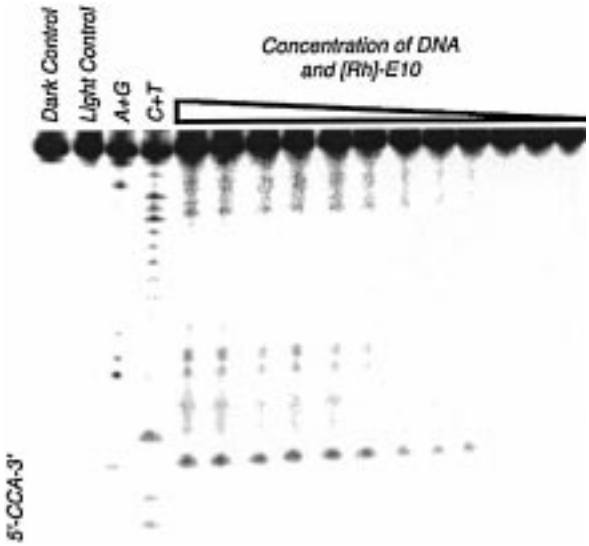

FIGURE 4: Autoradiogram of dissociation constant determination of [Rh]−E10 for 5′-CCA-3′ by photocleavage titration. Conditions: 3:1 ratio of hairpin oligonucleotide−metallointercalator or metallointercalator−peptide conjugate, 5 mM $MnCl_2$, 50 mM sodium cacodylate buffer, pH 7.0, 55 °C. The sequence of the hairpin oligonucleotide was 5′-AATT**CCA**CACAATTTTTTTGT-G**TGG**AATT-3′.

The origin of the enhanced DNA sequence selectivity of metallointercalator−peptide conjugates at elevated temperature was investigated by comparing the dissociation constants of [Rh]−E10 at 23 and 55 °C with a second hairpin oligonucleotide that contained the target sequence 5′-CCA-3′. Cleavage isotherms generated from autoradiograms of photocleavage titration gel electrophoresis experiments revealed an increased affinity at elevated temperature (Figure 6). Determination of the dissociation constants derived from the cleavage isotherms indicated that [Rh]−E10 binds 5-fold more tightly at 55 °C ($K_d = 2.3 \times 10^{-7}$ M) than at 23 °C ($K_d = 1.2 \times 10^{-6}$ M) to the 5′-CCA-3′ site.

DISCUSSION

DNA Recognition by Metallointercalator−Peptide Conjugates. We have synthesized and characterized a family of

Table 2: Summary of DNA Recognition by Peptide Conjugates of $[Rh(phi)_2(phen')]^{3+}$

conjugate	peptide sequence[a]	DNA site (s)[a]	K_d[b] ($\times 10^8$ M)
[Rh]−E6	$[Rh(phi)_2(phen')]^{3+}$−AANVA**E**AAWARAA-$CONH_2$	5′-AC**A**−3′, weak 5′-TC**A**−3′	9.9 ± 1.2
[Rh]−E10	$[Rh(phi)_2(phen')]^{3+}$−AANVAIAAW**E**RAA-$CONH_2$	5′-CC**A**−3′	5.7 ± 0.12
[Rh]−E6E10	$[Rh(phi)_2(phen')]^{3+}$−AANVA**E**AAW**E**RAA-$CONH_2$	weak 5′-CC**A**−3′	3.0 ± 0.5
[Rh]−R6A10	$[Rh(phi)_2(phen')]^{3+}$−AANVA**R**AAWARAA-$CONH_2$	consistent with 5′-(G/T)C**A**-3′	

[a] The primary photocleavage site is indicated in boldface type. [b] Dissociation constants were measured at 55 °C in the presence of 5 mM $MnCl_2$, except for [Rh]−E6E10, which was measured in the absence of $MnCl_2$. The dissociation constant of $[Rh(phi)_2(phen')]^{3+}$ for random-sequence DNA is $(7.0 \pm 0.5) \times 10^{-7}$ M.

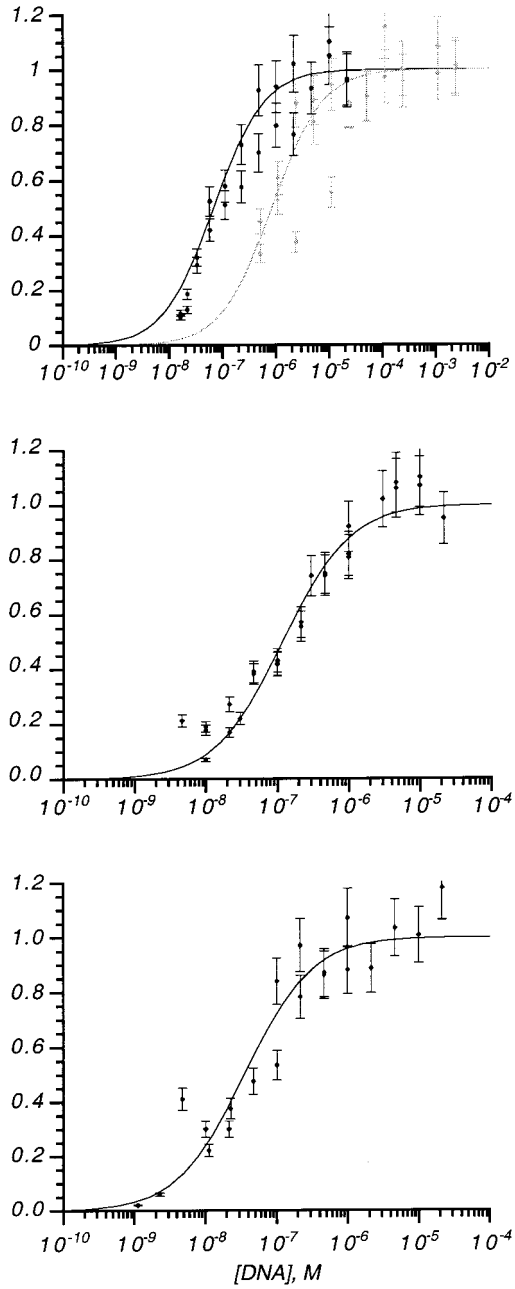

FIGURE 5: Isotherms indicating photocleavage intensity as a fraction of the maximum photocleavage intensity at the target site as a function of [DNA] for [Rh]−E10 (black, $K_d = 5.7 \times 10^{-8}$ M) and $[Rh(phi)_2(phen')]^{3+}$ (gray, $K_d = 7.0 \times 10^{-7}$ M) (top), [Rh]−E6 ($K_d = 9.9 \times 10^{-8}$ M) (center), and [Rh]−E6E10 ($K_d = 3.0 \times 10^{-8}$ M) (bottom). Conditions were as follows: (Top) 3:1 ratio of hairpin oligonucleotide−metallointercalator or metallointercalator−peptide conjugate, 5 mM $MnCl_2$, 50 mM sodium cacodylate buffer, pH 7.0, 55 °C. The hairpin oligonucleotide 5′-AGAGCCACGAGATTTTTTCTCGTGGCTCT-3′ was employed for [Rh]−E10 and $[Rh(phi)_2(phen')]^{3+}$. An additional hairpin oligonucleotide, 5′-AATTCCACACAATTTTTTTGTGTGGAATT-3′, was employed for $[Rh(phi)_2(phen')]^{3+}$. (Center) 3:1 ratio of hairpin oligonucleotide−metallointercalator−peptide conjugate, 5 mM $MnCl_2$, 50 mM sodium cacodylate buffer, pH 7.0, 55 °C. The hairpin oligonucleotide employed was 5′-AGAGACACGAGATTTTTTCTCGTGTCTCT-3′. (Bottom) 3:1 ratio of hairpin oligonucleotide−metallointercalator−peptide conjugate, 50 mM sodium cacodylate buffer pH 7.0, 55 °C. The hairpin oligonucleotide employed was 5′-AGAGCCACGAGATTTTTTCTCGTGGCTCT-3′.

metallointercalator−peptide conjugates. Screening of this family for sequence-selective DNA cleavage by use of the

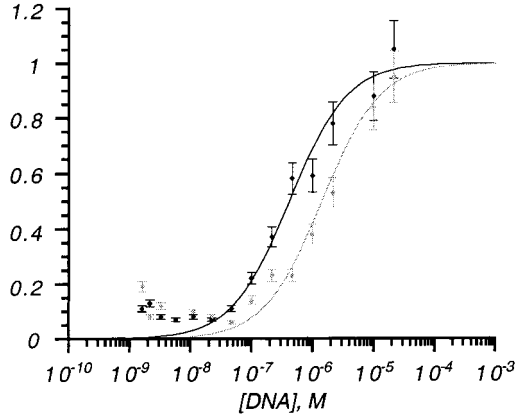

FIGURE 6: Temperature dependence of the dissociation constant of [Rh]−E10 for 5′-CCA-3′. Shown is the plot of relative photocleavage intensity as a function of [DNA]. Conditions: 3:1 ratio of hairpin oligonucleotide−[Rh]−E10, 5 mM $MnCl_2$, 50 mM sodium cacodylate buffer pH 7.0, 23 °C (gray, $K_d = 1.2 \times 10^{-6}$ M) or 55 °C (black, $K_d = 2.3 \times 10^{-7}$ M). The hairpin oligonucleotide employed was 5′-AATTCCACACAATTTTTTTGTGTGGAATT-3′.

^{32}P-end-labeled *Eco*RI/*Pvu*II 180-mer restriction fragment of pUC18 identified the new sequence-selective metallointercalator−peptide conjugates [Rh]−E6 (5′-ACA-3′), [Rh]−E6E10 (weak 5′-CCA-3′), and [Rh]−R6A10 (5′-(T/G)CA-3′). Changing the location of Glu^{10} to position 6 results in a change in selectivity from 5′-CCA-3′ to 5′-ACA-3′. Substitution of arginine for glutamate at position 6 causes additional changes in sequence preference.

Energetics of DNA Binding by [Rh]−E10. The affinity of metallointercalator−peptide conjugates for specific sites is a function of the metal complex and the appended peptide. Previously, we estimated the contribution of the peptide to specific binding as ≥1 kcal·mol^{-1} on the basis of the cleavage intensities of [Rh]−E10 and $[Rh(phi)_2(phen')]^{3+}$ at a 5′-CCA-3′ site, and we observed that a 100-fold excess of free peptide was incapable of competing with [Rh]−E10 for the DNA target (*9*). Comparison of the dissociation constant of [Rh]−E10 for a 5′-CCA-3′ sequence and the dissociation constant of $[Rh(phi)_2(phen')]^{3+}$ for random-sequence DNA at 55 °C in the presence of 5 mM $MnCl_2$ affords a similar value of 1.7 kcal·mol^{-1} for the energetic advantage of specific complex formation.

Comparable values have been reported for the energetic stabilization of specific complex formation by dimeric peptides derived from GCN4. Talanian et al. (*20*, *21*) found that the disulfide-linked dimer of a 31-mer peptide bound to the GCN4 recognition element with a K_d of 5×10^{-8} M. Similarly, Cuenoud and Schepartz (*22*) reported that an iron(II) bis(terpyridyl) dimer of a 29-mer peptide bound to the GCN4 recognition element with a K_d of 1.3×10^{-7} M. These values correspond to free energies of complex formation of −10.2 kcal·mol^{-1} (0.17 kcal·mol^{-1} per amino acid residue) and −9.6 kcal·mol^{-1} (0.17 kcal·mol^{-1} per amino acid residue), respectively. Remarkably, the energetic advantage of specific complex formation for [Rh]−E10 corresponds to a value of 0.13 kcal·mol^{-1} per amino acid residue, despite the small size and minimal secondary structure of the peptide.

DNA binding proteins derive most of their binding affinity from a combination of nonspecific electrostatic and hydrogen-

bonding interactions. Sequence discrimination is achieved through contacts made primarily by side chains of amino acid residues contained in a modular recognition domain. Our results indicate that, like DNA binding proteins, [Rh]−E10 derives the majority of its free energy of binding from a fairly sequence-neutral interaction (intercalation), while base-specific interactions between the E10 peptide and the target DNA sequence provide sequence discrimination.

The specificity of metallointercalator−peptide conjugates is a function of the ratio between the dissociation constant for the target site and the dissociation constants for nontarget sites. Photocleavage results of metallointercalator conjugates containing peptides derived from the P_{22} repressor demonstrated that optimal selectivity in DNA binding is observed at elevated temperature (*9*). In principle, either an increase in the affinity of the conjugate for the target sequence or a decrease in the affinity of the conjugate for nontarget sequences could afford the observed increase in specificity with increasing temperature. To distinguish between these possibilities, the effect of an increase in the temperature on the dissociation constant of [Rh]−E10 for its target site was determined. We find here that the metallointercalator−peptide conjugate binds 5-fold *more* tightly at 55 °C than at 23 °C. A similar increase in affinity at elevated temperatures was reported in calorimetric studies of glucocorticoid receptor binding to target DNA sites. The authors postulated that release of ordered water at the transcription factor−response element interface was responsible for the observed thermodynamic data (*23*, *24*).

Models for DNA Recognition. Previous work demonstrated that Glu^{10} is critical to recognition of 5′-CCA-3′ by [Rh]−E10 (*9*). Hydrogen-bonding contacts between the glutamate side-chain carboxylate and N4 of cytosine are a common recognition motif in crystal structures of protein−DNA complexes (*25*, *26*). Moreover, there is a correlation between specificity and helical content for a family of metallointercalator−peptide conjugates that target 5′-CCA-3′. Consequently, we previously proposed (*9*) a model for DNA recognition by [Rh]−E10 and related metallointercalator−peptide conjugates in which the peptide adopts a helical conformation upon DNA binding, and Glu^{10} makes base-specific contact with the 5′-cytosine of the 5′-CCA-3′ recognition site. With the data reported here, this model is refined.

Many amino acids with functional side chains are capable of making base-specific contacts with more than one type of base (*1*, *2*). However, DNA binding proteins can specify their target sites with single-base accuracy. Although the factors that determine which of several possible bases will be specified by a given amino acid in a given recognition domain are not clear, it has been suggested that the position and orientation of the peptide backbone with respect to the DNA determines the types of contacts that individual amino acids are capable of making. For recognition of a given nucleotide by a given amino acid, then, certain positions and orientations of the peptide backbone with respect to the DNA are preferred (*27*). Thus, we may estimate the position of the glutamate side chains of the [Rh]−E6 and [Rh]−E10 relative to their DNA target sites on the basis of the observed sequence selectivity.

Our refined model (Figure 7) was constructed by energy minimization with the following restraints: (i) the DNA was constrained to adopt canonical B-form torsion angles, except at the intercalation site; (ii) the DNA structural parameters (helical twist and helix rise) at the intercalation site, and the position of the intercalated phi ligand, were derived from the solution structure of Δ-α-[Rh[(*R*,*R*)-Me_2trien]phi]$^{3+}$ bound to 5′-TGCA-3′ (*28*, *29*); (iii) the relative position of the glutamate side-chain carboxylate and the 5′-cytosine of the 5′-CCA-3′ recognition site was constrained to match the relative position of Glu^{180} and its target cytosine in the *Escherichia coli* CAP protein−DNA complex (*30*); and (iv) the initial conformation of the peptide was a canonical α-helix. A similar analysis was performed for [Rh]−E6, with the relative position of the glutamate side-chain carboxylate and the cytosine of the 5′-ACA-3′ recognition site constrained to match the relative position of Glu^{180} and its target cytosine in the *E. coli* CAP protein−DNA complex. For simplicity, the Δ configuration of the rhodium center was employed throughout these modeling experiments; however, we have previously demonstrated that both diastereomers of peptide conjugates of [Rh(phi)$_2$(phen′)]$^{3+}$ bind to target DNA sequences with similar affinity, perhaps due to the inherent flexibility of the glutaryl linker (*9*).

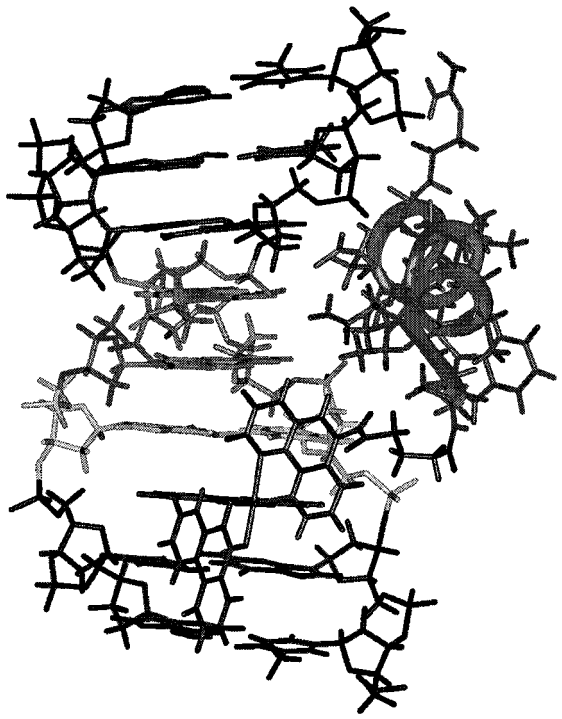

FIGURE 7: Model for DNA recognition by [Rh]−E10. Base pairs recognized by [Rh]−E10 are shown in light gray. For the respective metallointercalator−peptide conjugates, all of the structures were essentially identical.

From this model, we may draw inferences about the nature of contacts other than those made by glutamate side chains that contribute to sequence specificity. In our model of the [Rh]−E10−DNA complex, we observe that only the side chain of Ile^6 is capable of making a contact with the major-groove surface of the C·G base pair in the center of the 5′-CCA-3′ recognition site. Because this side chain possesses no functionality, sequence selectivity from such a contact would necessarily arise from shape complementarity. In our model of the [Rh]−E6−DNA complex, we observe that only alanine side chains lie on the face of the putative α-helix

positioned in the major groove, which is consistent with the observed preference for a thymine base on one of the strands at the 5′-terminus of the 5′-ACA-3′ recognition site.

Effect of the E6R Mutation on DNA Sequence Selectivity. Glu^6 of [Rh]−E6 is predicted to contact the central base pair of the 5′-ACA-3′ recognition site. However, replacing Glu^6 with Arg results in a change in the apparent consensus sequence from 5′-ACA-3′ to 5′-(T/G)CA-3′. Thus, the E6R modification causes a change in sequence preference at a base pair *adjacent* to the one considered to be contacted by Glu^6. Moreover, unlike [Rh]−E6 and [Rh]−E10, [Rh]−R6A10 does not afford a consistent asymmetry of strand cleavage and [Rh]−R6A10 appears to recognize some sequences that differ from its consensus sequence at one of the three base pairs. How can a single amino acid change cause such a complex change in the photocleavage characteristics of a metallointercalator−peptide conjugate? Some insight may be obtained by analysis of contacts between C·G base pairs and arginine and glutamate side chains in cocrystal structures of protein−DNA complexes (*31*). For example, C_α of Glu^{180} of the *E. coli* CAP protein lies on the cytosine side of the guanine−cytosine interface along the base pair axis and to the 5′-side of the contacted base. In contrast, C_α of Arg^{466} of the glucocorticoid receptor−DNA complex lies to the guanine side of the guanine−cytosine interface. After superimposition of the cytosine bases of the C·G base pairs contacted, the distance between C_α of Arg^{466} in the glucocorticoid receptor−DNA complex and C_α of Glu^{180} in the *E. coli* CAP protein−DNA complex is 6.4 Å. Such a difference between the preferred position of the C_α of Glu^6 of [Rh]−E6 and Arg^6 of [Rh]−R6A10 relative to the C·G base pairs they contact would produce a significant shift in the position of the α-helix relative to the DNA. This shift would affect both the amino acid side chain(s) that are presented to the base pair at the 5′-position of the recognition sequence and the position of the metal complex in the intercalation site. Consequently, both the sequence preferences at the 5′-position of the recognition sequence and the photocleavage characteristics of the metallointercalator−peptide conjugate could be perturbed. This result is consistent with the observation that multiple amino acids may be used to recognize a given base, and multiple bases may be recognized by the same amino acid.

Implications for Metallointercalator−Peptide Design. These metallointercalator−peptide conjugates permit the DNA recognition characteristics of individual amino acids to be studied in the context of a small, readily synthesized, well-defined system. By this approach, the recognition of DNA target half-sites by monomeric peptides may be investigated. In this study, we have examined the ability of a glutamate residue to effect sequence-selective DNA recognition, and we have compared the recognition characteristics of glutamate, arginine, and isoleucine at position 6 and the recognition characteristics of alanine and glutamate at position 10 in oligopeptides derived from the P_{22} repressor recognition α-helix. What we observe are interactions perhaps as complex as those seen in protein−DNA recognition. Here, too, single changes in amino acid residues can produce multiple changes in the base sequence targeted. While the application of small peptides to effect specific recognition should simplify many of the issues that govern protein−DNA interactions, at the same time, these smaller peptides lack the structural constraints and control that may be needed for predictive design.

Nonetheless an array of metallointercalator−peptide conjugates may be prepared that differ somewhat in sequence selectivity. Previously, we have reported that conjugates of $[Rh(phi)_2(bpy')]^{3+}$ with zinc-binding peptides can hydrolyze the phosphodiester backbone of DNA (*32*). Appending oligopeptides that confer site-specific DNA recognition to these complexes affords the possibility of carrying out these reactions in a sequence-selective fashion.

ACKNOWLEDGMENT

We thank the Biopolymer Synthesis and Analysis Center at Caltech for their technical assistance.

REFERENCES

1. Pabo, C. O., and Sauer, R. T. (1992) *Annu. Rev. Biochem. 61*, 1053.
2. Rhodes, D., Schwabe, J. W. R., Chapman, L., and Fairall, L (1996) *Philos. Trans. R. Soc. London B 351*, 501.
3. Desjarlais, J. R., and Berg, J. M. (1992) *Proc. Natl. Acad. Sci. U.S.A. 89*, 7345.
4. Choo, Y., and Klug, A. (1994) *Proc. Natl. Acad. Sci. U.S.A. 91*, 11168.
5. Nardelli, J., Gibson, T., and Charnay, P. (1992) *Nucleic Acids Res. 20*, 4137.
6. Desjarlais, J. R., and Berg, J. M. (1992) *Proteins: Struct., Funct., Genet. 12*, 101.
7. Thukral, S. K., Morrison, M. L., and Young, E. T. (1992) *Mol. Cell Biol. 12*, 2784.
8. Choo, Y., Sánchez-García, I., and Klug, A. (1994) *Nature 372*, 642.
9. Sardesai, N. Y., Zimmerman, K., and Barton, J. K. (1994) *J. Am. Chem. Soc. 116*, 7502.
10. Sardesai, N. Y., Lin, S. C., Zimmermann, K., and Barton, J. K. (1995) *Bioconjugate Chem. 6*, 302.
11. Sardesai, N. Y., and Barton, J. K. (1997) *J. Biol. Inorg. Chem. 2*, 762.
12. Sitlani, A., Long, E. C., Pyle, A. M., and Barton, J. K. (1992) *J. Am. Chem. Soc. 114*, 2303.
13. Caruthers, M. H., Barone, A. D., Beaucage, S. L., Dodds, D. R., Fisher, E. F., McBride, L. J., Matteucci, M., Stabinsky, Z., and Tang, J.-Y. (1987) *Methods Enzymol. 154*, 287.
14. Maniatis, T., Fritsch, E. F., and Sambrook, J. (1982) *Molecular Cloning*, Cold Spring Harbor Laboratory, Cold Spring Harbor, NY.
15. Maxam, A. M., and Gilbert, W. (1977) *Proc. Natl. Acad. Sci. U.S.A. 74*, 560.
16. Lohmann, T. M., and Mascotti, D. P. (1992) *Methods Enzymol. 212*, 400−424.
17. Winzor, D. J., and Sayer, W. H. (1995) *Quantitative Characterization of Ligand Binding*, Wiley-Liss, New York.
18. B. A. Jackson, C. A. Hastings, B. P. Hudson, T. Johann, and J. K. Barton, unpublished results.
19. Dauber-Osguthorpe, P., Roberts, V. A., Osguthorpe, D. J., Wolff, J., Genest, M., and Hagler, A. T. (1988) *Proteins: Struct., Funct., Genet. 4*, 31.
20. Talanian, R. V., McKnight, C. J., and Kim, P. S. (1990) *Science 249*, 769.
21. Talanian, R. V., McKnight, C. J., Rutkowski, R., and Kim, P. S. (1992) *Biochemistry 31*, 6871.
22. Cuenoud, B., and Schepartz, A. (1993) *Science 259*, 510.
23. Lündback, T., Zilliacus, J., Gustaffson, J.-Å., Carlstedt-Duke, J., and Härd, T. (1994) *Biochemistry 33*, 5955.
24. Lündback, T., and Härd, T. (1996) *Proc. Natl. Acad. Sci. U.S.A. 93*, 4754.

25. Schultz, S. C., Shields, G. C., and Steitz, T. A. (1991) *Science 253*, 1001.
26. Raskin, C. A., Diaz, G., Joho, K., and McAllister, W. T. (1992) *J. Mol. Biol. 228*, 506.
27. Pomerantz, J. L., Pabo, C. O., and Sharp, P. A. (1995) *Proc. Natl. Acad. Sci. U.S.A. 92*, 9752.
28. Hudson, B. P., Dupureur, C. M., and Barton, J. K. (1995) *J. Am. Chem. Soc. 117*, 9379.
29. Hudson, B. P., and Barton, J. K. (1998) *J. Am. Chem. Soc. 120*, 6877−6888.
30. Parkinson, G., Wilson, C., Gunasekera, A., Ebright, Y. W., Ebright, R. E., and Berman, H. M. (1996) *J. Mol. Biol. 260*, 395.
31. Luisi, B. F., Xu, W. X, Otwinowski, Z., Freedman, L. P., Yamamoto, K. R., and Sigler, P. B. (1991) *Nature 352*, 497.
32. Fitzsimons, M. P., and Barton, J. K. (1997) *J. Am. Chem. Soc. 119*, 3379.
33. Chen, Y. H., Yang, J. T., and Martinez, H. M. (1972) *Biochemistry 11*, 4120.
34. Lehrman, S. R., Tuls, J. L., and Lund, M. (1990) *Biochemistry 29*, 5590.

BI982039A